Large-Scale Modeling of Urban Nonpoint Source Pollution Using a Geographic Information System

Abstract
Concern about nonpoint source pollution associated with urban storm water has led to the development of new tools for better water quality planning. This paper presents an application of a geographic information system (GIS) for urban water quality study. The GIS was used to manage land-use data for nonpoint source pollution modeling and to aggregate pollutant loadings within various types of geographic units. An empirical water quality model was used to estimate pollutant loadings based primarily on land use. A land-use coverage was created by updating an old coverage through interpretation of recent photography. This land-use coverage was also used to record all pollutant loadings for each land-use polygon. Storm sewer maps were digitized and interpreted to create a coverage of storm sewer basins and sub-basins. By overlaying pollutant loadings with the sewer sub-basin layer, aggregated pollutant loadings for major sewer outfalls were calculated. Based on the loading information, critical areas of excessive pollutant loadings were located and the effectiveness of Best Management Practices (BMPs) to control pollutant loadings were evaluated.

Introduction
Nationwide, investigators have shown that nonpoint source pollution from urban areas is a major contributor to water quality degradation. Storm runoff and combined sewer overflows are the most significant nonpoint sources in urban areas (Peirce, 1980). Establishing the best control strategy for urban nonpoint source pollution includes initial assessment of the magnitude of the nonpoint source problem. This assessment must be geographically specific to effectively target control practices. Currently, empirical models are typically used to generate urban nonpoint source pollutant loadings. These models are based on the fact that urban nonpoint source pollution is mainly a function of land uses and associated activities (e.g., medium density residential, or highly impervious downtown commercial areas). Coefficients for pollutant loadings by land use have been developed from statistical analysis of field sampled data from the gamut of land uses found in urban areas. Therefore, the validity of model results depends on the resolution of land-use data and the specificity of land-use categories.

Modeling urban nonpoint source pollution across extensive urban areas requires a large number of units of analysis (land-use polygons) and resulting pollutant loadings because of highly heterogeneous land uses. It is crucial in urban nonpoint source studies to delineate the boundaries of different land uses, at least to the street block level, in order to effectively target control efforts. A procedure which facilitates nonpoint source modeling based on the aggregation of loadings from small, homogeneous areas provides detailed information about the contribution of nonpoint pollutants from specific areas in order to identify problems. We have called this a "micro" approach (Kim and Ventura, 1993). Such a micro-approach, using a high degree of spatial resolution for land-use data across extensive areas, has only been evaluated in much smaller urban areas.

A GIS provides the capabilities to integrate and display several types of geographic information in the micro-approach to urban nonpoint source modeling. This project tested three potential advantages of a GIS. First, existing digital layers representing street blocks can be imported and used as a base map and reference to collect pollutant loadings. This can also provide a framework for urban storm sewer collection area delineations. Second, parameters such as land use can be transferred between models and databases more easily using GIS data management functions. In particular, empirical models can be easily linked to GIS layers because coefficients can readily be applied to GIS layers (Sasowsky and Gardner, 1991). This implies that modeling procedures can be simplified, with less data processing time compared to manual methods. Third, aggregated pollutant loadings can be obtained for major sewer outfalls and other geographic units of aggregation through overlay analysis. This process will identify critical areas contributing a significant amount of pollutants. With additional geographic data such as land ownership and value, the GIS and nonpoint source model can be used to evaluate the cost and effectiveness of alternative control strategies in critical areas (Prey *et al.*, 1993). This should lead to best-fit control strategies, meeting the recent federal urban storm water regulations which require permits for certain categories of storm water discharges (U.S. Environmental Protection Agency, 1990).

In a previous Wisconsin Department of Natural Resources (WDNR) sponsored pilot study using a small urban area, Harris *et al.* (1991) concluded that remote sensing and GIS technologies provided reliable and timely data for urban nonpoint source pollution planning. The GIS provided a detailed base layer for identifying small land-use polygons, while TM satellite imagery and NHAP2 aerial photography provided an effective source of up-to-date land-use data. Kim *et al.* (1992) reported on the development and testing of the micro-approach in this relatively small urban area. The investigators also emphasized further study, i.e., applying the results from the pilot study to larger urban areas. Based on this study,

Photogrammetric Engineering & Remote Sensing,
Vol. 59, No. 10, October 1993, pp. 1539–1544.

0099-1112/93/5910–1539$03.00/0

Kyehyun Kim
Stephen Ventura
Environmental Remote Sensing Center, University of Wisconsin, 1225 West Dayton Street, Madison, WI 53706.

the WDNR initiated a large scale urban nonpoint source study for the Kinnickinnic River priority watershed. This study, as reported herein, was focused on developing a GIS-based nonpoint source modeling procedure to estimate pollutant loadings and establish effective mitigation strategies.

The major aim of this project was to link a GIS with a nonpoint source model for establishing effective BMPs based on model output of pollutants. The specific goals were (a) to acquire recent land use information and develop a GIS coverage; (b) to generate a sewer pipe network and delineate storm sewer sub-basin boundaries for use as pollutant loading boundaries of major sewer outfalls; (c) to estimate aggregated pollutant loadings of major sewer outfalls; and (d) to locate critical areas and establish BMPs for reducing pollutant loadings from these areas.

Study Area

The study area is an urban area in the southern part of Milwaukee County, Wisconsin (Figure 1). Most of the area drains into the Kinnickinnic River, while a small portion drains directly into Lake Michigan. The area has seven major streams and an urban storm sewer basin of about 27 mi² extending over parts of six municipalities, including the City of Milwaukee. The study area has a high density of intensive land uses, including large commercial and industrial areas, and a significant area in transportation such as freeways, railroads, and an airport.

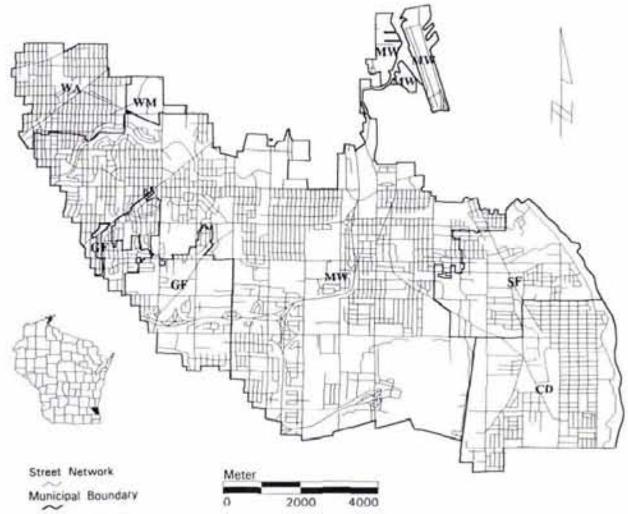

Figure 1. Street network and municipal boundaries of the study area. Displays street network imported from 1983 USGS DLG (1:100,000 scale) and boundaries of six municipalities: Milwaukee (**MW**), Cudahy (**CD**), St. Francis (**SF**), Green Field (**GF**), and West Allis (**WA**).

Methods

Land-Use Data Sources

Several different sources of land-use data were acquired for this project. In an effort to generate a recent land-use layer in an effective way, they were evaluated alone and in combination. These data sources were

- *SEWRPC land-use data.* 1985 land-use data in hard copy plot at a scale of 1:24,000 was purchased from the Southeastern Wisconsin Regional Planning Commission (SEWRPC) and used as a baseline to generate land-use data. A digital copy of these data could not be obtained in time for this study.
- *USGS DLG.* 1983 USGS Digital Line Graph (DLG) transportation layer at a scale of 1:100,000 was used to delineate detailed street and railroad networks. Check plots against more accurate data showed that the spatial accuracy of these data far exceeded national map accuracy standards for 1:100,000-scale material, and approached that of 1:24,000-scale material.
- *Aerial Photography.* 1:4,800-scale black-and-white lithographic copies of 1:20,000-scale aerial photographs from 1990 were purchased from SEWRPC. These were used in conjunction with the 1985 SEWRPC land-use coverage to generate recent land-use data. It had previously been determined that satellite imagery did not have sufficient resolution to support this application (Ventura and Harris, 1993).

Land-Use Generation

Land-use data were compiled based on a version of level III USGS urban land-use categories (Anderson, 1976) modified for inclusion in a nonpoint source model. Using the DLG layer, SEWRPC hard copy plot, and 1990 airphotos, a recent land-use coverage was generated. The steps used to generate land-use data were

- import street and railroad center lines from the USGS 1:100,000-scale DLG;
- digitize freeway and airport polygons from SEWRPC plot, transform these polygons to overlay on street center line coverage, and "dissolve" street center lines inside freeway, railroad and airport polygons;
- combine street center line and freeway coverages to form a polygonal coverage of street blocks and other transportation polygons. These blocks were then the initial basis for land-use interpretation; and
- generate a check-plot of the land-use block coverage at the scale of the SEWRPC plot. Note and add any additional line work such as when a block is sub-divided by two or more land uses of significant area.

The detailed land-use classes were assigned to individual land-use polygons using various sources of data in the following sequence:

- code freeways and railroads, primarily using SEWRPC plot;
- code open space, water bodies, and parks primarily using 1:24,000-scale quadrangle maps, supplemented by SEWRPC plot and airphotos;
- code institutional uses such as schools and hospitals, using all three data sources; and
- code commercial, industrial, and residential areas by initially assigning land uses to broad areas according to the SEWRPC plot and then using the 1990 airphotos to validate and refine. In other words, the SEWRPC data were used to delineate major land-use boundaries, and then block-by-block interpretations were made with the photography, such as determining residential density.

Storm Sewer Sub-Basin Generation

To delineate the pollutant loading boundaries of major sewer outfalls, a storm sewer pipe network coverage was generated. This was done by digitizing storm sewer pipe maps provided by individual municipalities. The 74 sewer maps obtained from municipal engineering offices were delivered in various scales and degrees of quality. These maps were individually digitized to form line coverages. The City of Milwaukee was unique in that extensive interpretation of the sewer maps had to be done before digitizing, i.e., many pipes crossed, went in and out of drainage ditches, etc. The pipes were digitized in accordance with EPA's urban storm water regulations (Environmental Protection Agency, 1990). The minimum diameter of sewer pipes digitized was 36 inches in residential and 12 inches in commercial, industrial, and other areas. Zoning information, either on the storm sewer maps or from other sources, was used as a means to distinguish general land uses. Pipes smaller than the minimum diameter were not incorporated into the sewer network except as needed for hydrologic connectivity. These coverages were consolidated into one composite coverage to represent the sewer system of the entire study area (Figure 2).

The sewer sub-basins were delineated based on a hierarchical watershed delineation in three steps. The first step was to delineate two major boundaries for the Kinnickinnic River and Lake Michigan. The Kinnickinnic River has a watershed area of 21.3 mi², where 5.5 mi² drains directly to Lake Michigan. The second step was to delineate the boundaries of major tributaries (mainly those discharging into the Kinnickinnic River). The Kinnickinnic River has six tributaries, so it was further divided into six sub-watersheds (West Milwaukee Ditch, Cherokee Park Creek, Wilson Park Creek, Ville Mann Creek, Holmes Creek, and Lyons Park Creek) based on topography, surface drainage, and storm sewer network flow. The last step was to delineate individual sewer sub-basin boundaries by interpreting the storm sewer pipe network. This resulted in a coverage showing pollutant discharge boundaries for each sewer outfall.

A total of 97 sewer sub-basins, as shown in Figure 3, were delineated using the digitized sewer network, supplemented by the street coverage and topography from 1:24,000-scale quadrangle maps. The major goal in delineating the sewer sub-basins was to set the sewer sub-basin boundaries based on minimum end-pipe size to meet the EPA's requirement for storm water management. Therefore, delineation was done at a fine resolution, resulting in sewer sub-basins ranging from 11 to 1,008 acres in discharge area. This fine resolution makes it possible to establish well-suited BMPs for a variety of local urban conditions.

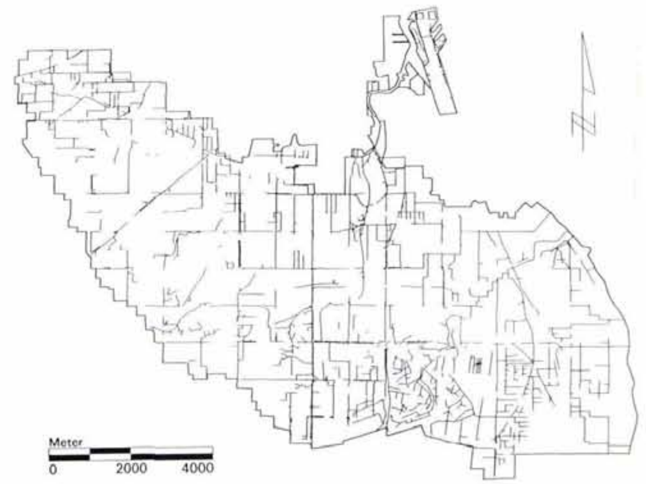

Figure 2. Digitized storm sewer network. Seventy-four sewer maps were digitized and individually registered into a Universal Transverse Mercator (**UTM**) coordinate system and integrated into a sewer network coverage.

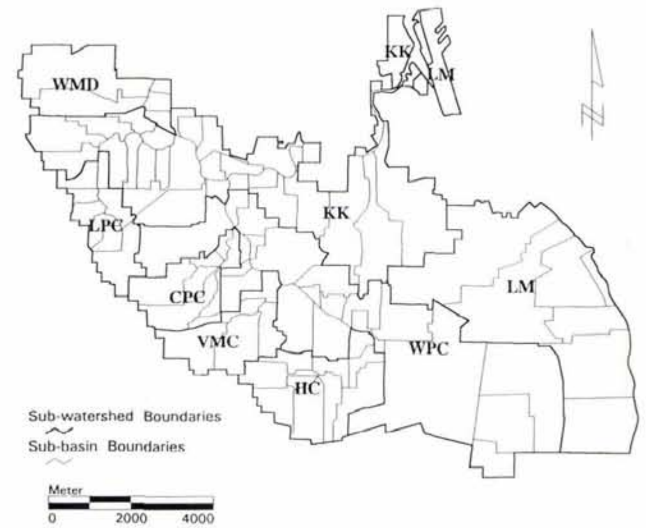

Figure 3. Sub-watershed and storm sewer sub-basin boundaries. Displays boundaries of 97 storm sewer sub-basins and eight sub-watersheds: West Milwaukee Ditch (**WMD**), Lyons Park Creek (**LPC**), Cherokee Park Creek (**CPC**), Ville Mann Creek (**VMC**), Holmes Creek (**HC**), Wilson Park Creek (**WPC**), Lake Michigan (**LM**), and Kinnickinnic River (**KK**).

Results

Land-Use Interpretation Accuracy

Establishing ground truth by drive-by inspection was conducted to analyze the accuracy of land-use interpretation. Over half the blocks (1440 out of 2789 polygons in the land-use coverage) were examined. Considering the relatively homogeneous make-up of residential areas and the relatively higher ratios of interpretation errors in commercial, industrial, and institutional classes, emphasis was given to the inspection of the latter classes. The results from the ground truth were used to refine the land-use data.

Interpretation accuracy was analyzed based on six major land-use categories and 22 detailed land-use classes. Due to the use of reference data provided by SEWRPC and large scale airphotos, the final coverage had a high interpretation accuracy. The six major categories show 98 percent overall accuracies (Table 1). The residential and transportation classes were almost 100 percent correct. The lowest accuracy was obtained for the industrial class. Some confusion between the industrial class and commercial and open space classes was observed. Not surprisingly, lower accuracies were noted for many sub classes. Relatively lower accuracy was obtained in low density and multi-family residential areas and office parks. Low density residential was often confused with medium density residential, and multi-family was confused with high density residential areas, as expected. The general land-use pattern of office parks is similar to strip commercial. This caused lower accuracy for office parks. The mobile home park, schools, airport, hospitals, water, cemetery, freeways, and railroad were 100 percent correct, mainly due to the use of topographic maps, which indicated the locations of several of these classes.

Nonpoint Source Modeling

An empirical urban water quality model developed by WDNR—Source Loading and Management Model (SLAMM)—was used to estimate the pollutant loadings of each land-use polygon. This model calculates runoff volumes and urban

Table 1. Land Use Interpretation Accuracy of Six Major Categories. Displays Interpretation Accuracy of Land Use in Six Major Categories. Also Shown Are Detailed Land-Use Classes of each Category and their Classification Accuracies.

Known Land Use Classes Sub-classes (% accuracy)	Number of Polygons	Accuracy (%)	Number of polygons classified into classes					
			Resi-dential	Comm-ercial	Indu-strial	Open space	Insti-tutional	Trans-portation
Residential	556	100	555	1				
High Density (96)								
Medium density (95)								
Low density (75)								
Multi-family (74)								
Mobile home (100)								
Commercial	299	96	8	287	2		2	
Strip commercial (95)								
Downtown commercial (93)								
Shopping center (80)								
Office park (70)								
Industrial	266	93		9	247	10		
Manufacturing (99)								
Light industry (82)								
Airport (100)								
Open Space	125	99			1	124		
Undeveloped (99)								
Construction (88)								
Park (84)								
Water (100)								
Cemetery (100)								
Institutional	113	98		1	1		111	
School (100)								
Miscellaneous (88)								
Hospital (100)								
Transportation	81	100						81
Ralroad (100)								
Freeway (100)								

pollutant loadings from individual rainfall events for each land-use type (Pitt, 1988). This model also allows the user to estimate reductions in pollutant loadings from source areas due to control measures such as detention ponds or infiltration devices (WDNR, 1991). The major parameters required for modeling are annual rainfall amount, soil type, existing control practices, pollutant loadings coefficients, and the acreage of each land use. In practice, acreages and land-use classes are the only independent variables in the modeling. Uniform values were used for the whole area for the other input data.

The strength of the SLAMM model is in the small storm hydrology algorithms and source area pollutant coefficients at the land-use sub-class level (WDNR, 1991). The small storm hydrology verification took place in Toronto, Ontario and Milwaukee, Wisconsin on 185 random rainfall events. The observed runoff volume was within 2 mm of model predicted runoff in most cases. The source area coefficients have been developed through extensive field calibration and verification, including an ongoing effort by WDNR to refine these values.

The model was run for 97 sub-basins of eight sub-watersheds. Loadings of six pollutants of concern were obtained from the model. Results from the sub-basin analyses were used to calculate total and unit (per acre) loadings for sub-watersheds and municipalities. Loadings from individual land-use polygons were stored as an additional attribute in that coverage. Through overlay analysis, it was possible to determine loadings within any larger division of the area.

Figure 4 shows the yearly and unit pollutant loadings of each sub-watershed. For heavy metals (e.g., lead, copper, zinc, and cadmium), Wilson Park Creek showed the highest loadings except phosphorus, followed by the Kinnickinnic and Lake Michigan sub-watersheds. This is explained by the large industrial area, including an airport, in Wilson Park Creek. The Kinnickinnic sub-watershed has the highest loadings of phosphorus, followed by Wilson Park Creek sub-watershed, due to its large residential area. The unit pollutant loading—the yearly pollutant loadings per acre — were highest for West Milwaukee Ditch. This was expected given the relatively high proportion of heavy industrial land use, the balance being largely residential with little open space. This area also has the highest unit loadings of sediment solids.

For individual municipalities, the City of Milwaukee shows the highest total pollutant loadings followed by the cities of Cudahy and West Allis. This was expected because the contributing area of Milwaukee is much larger than any other municipality. The unit pollutant loading analysis showed that the City of West Milwaukee had the highest per-acre loadings of all types of pollutants. This is due to its small area and relatively high portion of industrial land uses.

Best Management Practices

Based on the pollutant loading analysis, a critical sub-basin was selected for evaluation of BMPs. The KK26 sub-basin was selected in the east central part of Kinnickinnic sub-watershed because of its high pollutant loadings and relatively large portion of residential area. Wet ponds were the BMPs selected to reduce sediment loading in receiving bodies. The

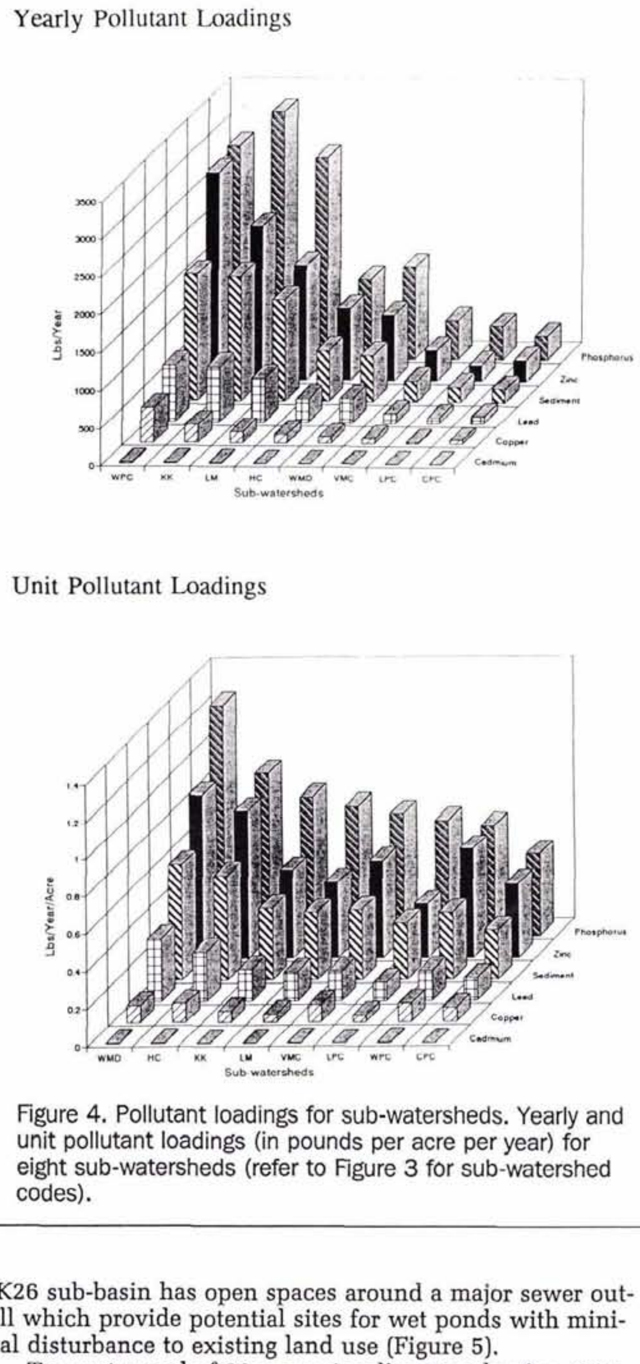

Figure 4. Pollutant loadings for sub-watersheds. Yearly and unit pollutant loadings (in pounds per acre per year) for eight sub-watersheds (refer to Figure 3 for sub-watershed codes).

KK26 sub-basin has open spaces around a major sewer outfall which provide potential sites for wet ponds with minimal disturbance to existing land use (Figure 5).

To meet a goal of 90 percent sediment reduction, DNR planners calculated a minimum wet pond size of 5.3 acres. Fortuitously, about 5.4 acres of open space was located near the outfall of this sub-basin, making the siting and implementation of BMPs a straightforward task. This example demonstrated that planners now have the tools and data to effectively target and evaluate BMPs.

Conclusion

This study demonstrates the potential application of a GIS for modeling purposes in water quality studies in a large urban area. The methods from this study should be applicable to other urban areas for establishing BMPs. The micro-approach can identify the magnitude of pollutant loadings from any size land-use polygon and provide the basis for aggregation to larger areas. This procedure will assist communities in meeting the EPA's storm water requirements.

No major problems existed in the linkage of model parameters between GIS data and the nonpoint source model. The model output, transferred back to individual land-use polygons, was effective for graphical display and for accumulating pollutant loadings to find critical pollution areas. This study demonstrates that GIS technology is effective for urban nonpoint source pollution control, using its data automation, overlay analysis, database management, and cartographic display capabilities.

Up-to-date, accurate data that were specific enough to support urban nonpoint source pollution modeling were generated from aerial photography in conjunction with other data. The aerial photography was used with existing DLG data to delineate individual urban street blocks. More specific land-use boundaries within street blocks were delineated using a 1985 SEWRPC land-use map. Considering the high accuracy of the land-use interpretation (over 90 percent using aerial photography), the procedure to generate land-use data demonstrated in this micro-approach could be further used for large scale urban nonpoint source pollution modeling for other urban areas.

The micro-approach has two time-consuming compo-

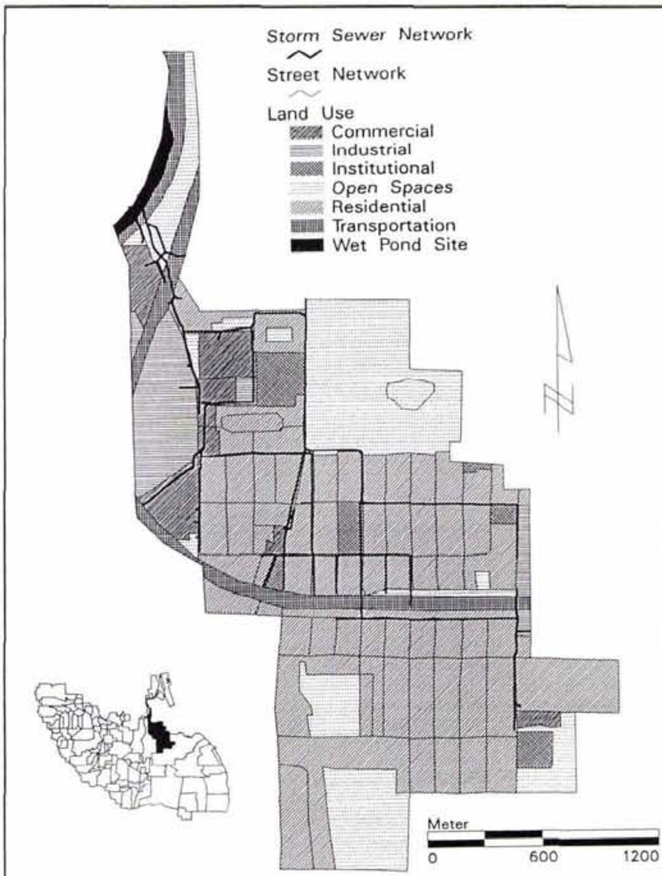

Figure 5. Critical sub-basin: KK26. Displays land-use inventory and storm sewer network of KK26 sub-basin selected as a critical sub-basin. A 5.4-acre open space around outfalls was used as a potential wet pond site for reducing suspended solids by 90 percent.

nents—manual land-use interpretation and boundary delineation of sewer sub-basins. The more these tasks can be automated, the more efficient the approach will be. Automated urban land-use generation using scanned aerial photography and computerized land-use classification methods such as texture based classifiers may offer an effective approach to mapping with high spatial resolution imagery (Kim, 1993). However, the cost of scanning and the high degree of technical expertise needed to classify images may preclude routine use by municipalities. Head-ups (on-screen) digitizing may be an effective way to realize some advantages of a GIS approach to land-use generation using known interpretation techniques.

For the delineation of sewer sub-basin boundaries, a more automated procedure could save time and effort. However, the initial automation of storm sewer maps will require a great deal of skilled interpretation if the variety and reliability of maps in the Milwaukee area is any indication. After initial data capture, it should be possible to develop rules based on topography, flow direction, and connectivity to automate the delineation of drainage basins. If these efforts are done in conjunction with the development of facilities management systems for storm sewers, additional benefits beyond water quality planning will accrue.

Acknowledgments

This project was done under Kinnickinnic River Priority Watershed contract number NRB-98029 from WDNR. Special thanks are due to water resource specialist of WDNR, Jeff Prey. Staff and students at the University of Wisconsin-Madison Land Information and Computer Graphics Facility contributed time and expertise to this project, including Pete Thum, Kristine Kuhlman, and Nan Liu.

References

Anderson, J. R., E. E. Hardy, J. T. Roach, and R. E. Witmer, 1976. *A Land Use and Land Cover Classification System for Use with Remote Sensing Data*, Geological Survey Professional Paper 964, U.S. Government Printing Office, Washington, D.C.

Harris, P. M., K. Kim, S. J. Ventura, T. G. Thum, J. Prey, 1991. Linking a GIS within Urban Nonpoint Source Pollution Model, *LIS/GIS Annual Proceedings*, American Society for Photogrammetry and Remote Sensing, Atlanta, Georgia, October.

Kim, K., 1993. *Object-Oriented Urban Classification Using Remote Sensing and Geographical Information System*, Ph.D. Dissertation. University of Wisconsin-Madison (in press).

Kim, K., and S. J. Ventura, 1993. Urban Nonpoint Source Pollution Assessment Using a Geographical Information System, *Journal of Environmental Management* (in press).

Kim, K., S. J. Ventura, P. M. Harris, and J. Prey, 1992. *A Micro Approach for Urban Nonpoint Source Pollution Assessment*, AWRA Wisconsin Chapter Conference—Land Use Impact on Water Quality, La Crosse, Wisconsin, March.

Peirce, J. J., 1980. Strategies to Control Nonpoint Source Water Pollution, *Water Resources Bulletin*, 16(2):220–225.

Pitt, R., 1988. *SLAMM 5. Source Loading and Management Model: An Urban Nonpoint Source Quality Model*, Ph.D. Dissertation, University of Wisconsin-Madison.

Prey, J. P., S. J. Ventura, and K. Kim, 1993. Storm Water Pollution Control Practices Siting and Retrofitting Within the Context of a GIS, *Proceedings-GIS'93*, Vancouver, B.C. (in press).

Sasowsky, K. C., and T. W. Gardner, 1991. Watershed Configuration and Geographical Information System Parameterization for SPUR Model Hydrologic Simulation, *Water Resources Bulletin*, 27(1):7–18.

U.S. Environmental Protection Agency (USEPA), 1990. *EPA Administered Permit Program; The National Pollutant Discharge Elimination Program*, Washington, D.C.

Ventura, S. J., and P. M. Harris, 1993. A Comparison of Classification Techniques for Urban Land Use Mapping, *GeoCarto International* (in press).

Wisconsin Department of Natural Resources (WDNR), 1991. *SLAMM Model Calibration and Example Application Project, Phase 1* Technical Memorandum Data Review and Verification, prepared by Warzyn, Inc., 38 p.

Kirk F. Adkins and *Carolyn J. Merry*, Accuracy Assessment of Elevation Data Sets Using the Global Positioning System.

Robert J. Andres and *William I. Rose*, Description of Thermal Anomalies on Two Active Guatemalan Volcanoes Using Landsat Thematic Mapper Imagery.

Peter August, Joanne Michaud, Charles LaBash, and *Christopher Smith*, GPS for Environmental Applications: Accuracy and Precision of Locational Data.

William L. Baker, Jimmie J. Honaker, and *Peter J. Weisberg*, Using Aerial Photography and GIS to Map the Forest-Tundra Ecotone in Rocky Mountain National Park, Colorado, for Global Change Research.

E. Ben-Dor, F. A. Kruse, A. B. Lefkoff, and *A. Banin*, Comparison of Three Calibration Techniques for Utilization of GER 63-Channel Aircraft Scanner Data of Makhtesh Ramon, Negev, Israel.

David W. Bolgrien, Nick G. Granin, and *Leo A. Levin*, Surface Temperature Dynamics of Lake Baikal Observed from AVHRR Images.

Paul V. Bolstad and *Timothy Stowe*, An Evaluation of DEM Accuracy: Elevation, Slope, and Aspect.

B. Brisco and *R. J. Brown*, Multi-Date SAR/TM Synergism for Crop Classification in Western Canada.

Daniel G. Brown and *Thaddeus J. Bara*, Recognition and Reduction of Systematic Error in Elevation and Derivative Surfaces from 7½-Minute DEMs.

Duane C. Brown, New Developments in Photogeodesy.

Keith C. Clarke, James A. Brass, and *Phillip J. Riggan*, A Cellular Automation Model of Wildfire Propagation and Extinction.

Marco D'Errico, Antonio Moccia, and *Sergio Vetrella*, High-Frequency Observation of Natural Disasters by SAR Interferometry.

C. Conese, M. A. Gilabert, F. Maselli, and *L. Bottai*, Topographic Normalization of TM Scenes through the Use of an Atmospheric Correction Method and Digital Terrain Models.

Liping Di and *Donald C. Rundquist*, A One-Step Algorithm for Correction and Calibration of AVHRR Level 1b Data.

Mary E. Dillworth, Jerry L. Whistler, and *James W. Merchant*, Measuring Landscape Structure Using Geographic and Geometric Windows.

Melanie Dutkiewicz and *Ian Cumming*, Evaluation of the Effects of Encoding on SAR Data.

Kathleen Edwards and *Philip A. Davis*, The Use of Intensity-Hue-Saturation Transformation for Producing Color Shaded-Relief Images.

Max J. Egenhofer, Pre-Processing Queries with Spatial Constraints.

L. Fent, R. J. Hall, and *R. K. Nesby*, Aerial Films for Forestry Inventory: Optimizing Film Parameters.

Peter F. Fisher, Visualization of the Reliability in Classified Remotely Sensed Images.

Giles M. Foody, Ordinal Level Classification of Sub-Pixel Tropical Forest Cover.

Giles M. Foody, Mary B. McCulloch, and *William B. Yates*, Classification of Remotely Sensed Data by an Artificial Neural Network: Issues Related to Training Data Characteristics.

Thomas D. Frank, Scott A. Tweddale, and *David E. Knapp*, Variability of At-Satellite Surface Reflectance from Landsat TM and NOAA AVHRR in Death Valley National Monument.

Steven E. Franklin, Discrimination of Subalpine Forest Species and Canopy Density Using Digital CASI, SPOT PLA, and Landsat TM Data.

Tung Fung and *King-chong Chan*, Spatial Composition of Spectral Classes: A Structural Approach for Image Analysis of Heterogeneous Land-Use and Land-Cover Types.

Sucharita Gopal and *Curtis Woodcock*, Theory and Methods for Accuracy Assessment of Thematic Maps Using Fuzzy Sets.

Armin Gruen and *Thomas P. Kersten*, Sequential Estimation in Robot Vision.

Barry N. Haack and *E. Terrance Slonecker*, Merged Spaceborne Radar and Thematic Mapper Digital Data for Locating Villages in Sudan.

Luoheng Han and *Donald C. Rundquist*, The Response of both Surface Reflectance and the Underwater Light Field to Various Levels of Suspended Sediments: Preliminary Results.

Kenneth C. Hardcastle, Photolineament Factor: A New Computer-Aided Method for Remotely Sensing the Degree to which Bedrock is Fractured.

Perry J. Hardin, Parametric and Nearest-Neighbor Methods for Hybrid Classification: A Comparison of Pixel Assignment Accuracy.

Perry J. Hardin and *David G. Long*, Discriminating between Tropical Vegetation Formations Using Reconstructed High-Resolution Seasat-A Scatterometer Data.

L. W. Harding, Jr., E. C. Itsweire, and *W. E. Esaias*, Algorithm Development for Recovering Chlorophyll Concentrations in the Chesapeake Bay Using Aircraft Remote Sensing, 1989-1991.

Paul M. Harris and *Stephen J. Ventura*, The Integration of Geographic Data with Remotely Sensed Imagery to Improve Classification in an Urban Area.

Christian Heipke, State-of-the-Art of Digital Photogrammetric Workstations for Topographic Applications.

Olaf Hellwich and *Wolfgang Faig*, Graph-Based Feature Matching Using Descriptive and Relational Parameters.

E. Hierholzer, Calibration of a Video Rasterstereographic System.

Cindy Hill Wilcox, Bruce E. Frazier, and *Shane T. Ball*, Relationship between Soil Organic Carbon and Landsat TM Data in Eastern Washington.

Kai-Yi Huang and *Paul W. Mausel*, Comparing a Piecewise Linear Classifier with Gaussian Maximum-Likelihood and Parallelepiped Classifiers in Terms of Accuracy and Speed.

Lucas L. F. Janssen and *J. M. van der Wel*, Accuracy Assessment of Satellite Derived Land-Cover Data: A Review.

Rachida Jazouli, David L. Verbyla, and *Dennis L. Murphy*, Evaluation of SPOT Panchromatic Digital Imagery for Updating Road Locations in a Harvested Forest Area.

Katarina Johnsson, Segment-Based Land-Use Classification from SPOT Satellite Data.

Doug King, Pat Walsh, and *Frank Ciuffreda*, Airborne Digital Frame Camera Imaging for Elevation Determination.

Karl Kraus, Visualization of the Quality of Surfaces and their Derivatives.

E. F. Lambin, J. A. Walkey, and *N. Petit-Maire*, Detection of Holocene Lakes in the Sahara Using Satellite Remote Sensing.

Christopher T. Lee and *Stuart E. Marsh*, The Use of Archival Landsat MSS and Ancillary Data in a GIS Environment to Map Historical Change in an Urban Riparian Habitat.

Jay Lee, Visibility Dominance and Topographic Features on Digital Elevation Models.

Donald L. Light, Moonsat: An Orbital Imaging System for Mapping the Moon.

E. J. Milton, Teaching Atmospheric Correction Using a Spreadsheet.

Douglas M. Muchoney and *Barry N. Haack*, Change Detection for Monitoring Forest Defoliation.

Janet E. Nichol, A GIS Based Approach to Microclimate Monitoring in Singapore's High Rise Housing Estate.

Kurt Novak, Mobile Mapping Technology for GIS Data Collection.

J. Olaleye and *W. Faig*, An Evaluation of Three M-Processor Designs for a Digital Photogrammetric System.

Ahmet Bahadir Orun and *Krishnaier Natarajan*, A Modified Bundle Adjustment Software for SPOT Imagery and Photography: A Tradeoff.

Richard A. Pries, A System for Large-Scale Image Mapping and GIS Data Collection.

Francis A. Roesch, Jr., *Paul C. Van Deusen*, and *Zhiliang Zhu*, A Comparison of Various Estimators for Updating Forest Area Coverage Using AVHRR and Forest Inventory Data.

Ken Rutchey and *Les Vilchek*, Development of an Everglades Vegetation Map Using a SPOT Image and the Global Positioning System.

H. T. Schreuder, *V. J. LaBau*, and *J. W. Hazard*, The Alaska Four-Phase Forest Inventory Sampling Design Using Remote Sensing and Ground Sampling.

Michael B. Smith and *Andrej Vidmar*, Data Set Derivation for GIS-Based Urban Hydrological Modeling.

I. Tannous and *B. Pikeroen*, Parametric Modeling of Spaceborne SAR Image Geometry Application: SEASAT/ SPOT Image Registration.

Prasad S. Thenkabail, *Andrew D. Ward*, *John G. Lyon*, and *Carolyn J. Merry*, Thematic Mapper Vegetation Indices for Determining Soybean and Corn Growth Parameters.

J. A. Thomasson, *C. W. Bennett*, *B. D. Jackson*, and *M. P. Mailander*, Differentiating Bottomland Tree Species with Multispectral Videography.

E. Lynn Usery, Virtual Stereo Display Techniques for Three-Dimensional Geographic Data.

Howard Veregin, Integration of Simulation Modeling and Error Propagation for the Buffer Operation in GIS.

Michael E. Wehde, Digital Image Comparison by Subtracting Contextual Transformations: Percentile Rank Order Differentiation.

Anthony G. Wiley and *Kam W. Wong*, Geometric Calibration of Zoom Lenses for Computer Vision Metrology

November Special Issue on GPS Photogrammetry

Sean Curry and *Karen Schuckman*, Practical Considerations for the Use of Airborne GPS for Photogrammetry.

I. Colomina, A Note on the Analytics of Aerial Triangulation with GPS Aerial Control.

F. Ackermann and *H. Schade*, Application of GPS for Aerial Triangulation.

Dean C. Merchant, GPS-Controlled Aerial Photogrammetry.

Robert L. Tudhope, Contract Issues for GPS/Photogrammetry: A Management Perspective.

A. Gruen, *M. Cocard*, and *H.-G. Kahle*, Photogrammetry and Kinematic GPS Results of a High Accuracy Test.

Karsten Jacobsen, Experience in GPS-Photogrammetry.

Rolf D. Becker and *Jean Pierre Barriere*, Airborne GPS for Photo Navigation and Photogrammetry (An Integrated Approach).

K. P. Schwarz, *M. A. Chapman*, *M. E. Cannon*, and *P. Gong*, An Integrated INS/GPS Approach to the Georeferencing of Remotely Sensed Data.

LIST OF "LOST" CERTIFIED PHOTOGRAMMETRISTS

We no longer have valid addresses for the following Certified Photogrammetrists. If you know the whereabouts of any of the persons on this list, please contact ASPRS headquarters so we can update their records and keep them informed of all the changes in the Certification Program. Thank you.

Jack R. Anthony	Franek Gajdeczka	Lawrence Johnson	Sherman Rosen
Dewayne Blackburn	George Glaser	Spero Kapelas	Lane Schultz
Gerard Borsje	William Grehn, Jr.	Andre J. Langevin	Keith Syrett
Albert Brown	Louis T. Harrod	Harry J. Miller	William Thomasset
Eugene Caudell	F.A. Hildebrand, Jr.	Marinus Moojen	Conrad Toledo
Robert Denny	James Hogan	M. David L. Morgan	Robert Tracy
			Lawrence Watson